Anomalous Composition-Induced Crossover in the Magnetic Properties of the Itinerant-Electron Antiferromagnet $Ca_{1-x}Sr_xCo_{2-y}As_2$

N. S. Sangeetha,[1] V. Smetana,[1,2] A.-V. Mudring,[1,2] and D. C. Johnston[1,3]

[1]*Ames Laboratory, Iowa State University, Ames, Iowa 50011, USA*
[2]*Department of Materials Science and Engineering, Iowa State University, Ames, Iowa 50011, USA*
[3]*Department of Physics and Astronomy, Iowa State University, Ames, Iowa 50011, USA*

The inference of Ying *et al.* [Europhys. Lett. **104**, 67005 (2013)] of a composition-induced change from c-axis ordered-moment alignment in a collinear **A**-type antiferromagnetic (AFM) structure at small x to ab-plane alignment in an unknown AFM structure at larger x in $Ca_{1-x}Sr_xCo_{2-y}As_2$ with the body-centered tetragonal $ThCr_2Si_2$ structure is confirmed. Our major finding is an anomalous magnetic behavior in the crossover region $0.2 \lesssim x \lesssim 0.3$ between these two phases. In this region the magnetic susceptibility vs temperature $\chi_{ab}(T)$ measured with magnetic fields **H** applied in the ab plane exhibit typical AFM behaviors with cusps at the Néel temperatures of ~ 65 K, whereas $\chi_c(T)$ and the low-temperature isothermal magnetization $M_c(H)$ with **H** aligned along the c axis exhibit extremely soft ferromagneticlike behaviors.

Much research since 2008 has focused on studies of iron-based layered pnictides and chalcogenides due to their unique lattice, electronic, magnetic and superconducting properties [1–6]. An important family of these materials is comprised of doped and undoped body-centered tetragonal parent compounds AFe_2As_2 ($A =$ Ca, Sr, Ba, Eu) with the $ThCr_2Si_2$-type structure (122-type compounds). The undoped and underdoped AFe_2As_2 compounds exhibit a tetragonal to orthorhombic distortion of the crystal structure at $T_S \lesssim 200$ K. They also exhibit itinerant collinear antiferromagnetic (AFM) spin-density-wave ordering at a temperature T_N the same as or slightly lower than T_S. The ordered moments in the stripe AFM structure of the orthorhombic phase are oriented in the ab plane. In 2014, a temperature T-induced AFM spin-reorientation transition to a new AFM C_4 phase was discovered in the hole-underdoped $Ba_{1-x}Na_xFe_2As_2$ system upon cooling below T_N that can coexist with superconductivity [7]. A subsequent investigation by polarized and unpolarized neutron diffraction determined that the ordered moments in the new phase are aligned along the c axis instead of along the ab plane as in the stripe AFM structure [8]. The work on the $Ba_{1-x}Na_xFe_2As_2$ system was followed by the observation of the same AFM C_4 phase in the $Ba_{1-x}K_xFe_2As_2$ [9–11], $Sr_{1-x}Na_xFe_2As_2$ [12,13], and $Ca_{1-x}Na_xFe_2As_2$ [14] systems. These results are important to understanding the mechanism of superconductivity and other aspects of the hole-doped iron arsenides [15–21].

A similar but composition-induced moment realignment was suggested to occur in the isostructural CoAs-based system $Ca_{1-x}Sr_xCo_{2-y}As_2$ [22]. $CaCo_{2-y}As_2$ has a so-called collapsed-tetragonal (cT) structure with As–As bonding along the c axis between adjacent CoAs layers

[23] and has $\approx 7\%$ vacancies on the Co sites [24,25]. It exhibits itinerant **A**-type AFM ordering below $T_N = 52$–77 K, depending on the sample, with the ordered moments of ≈ 0.3–0.4 $\mu_B/$Co (μ_B is the Bohr magneton) within an ab-plane Co layer aligned ferromagnetically (FM) along the c axis and with AFM alignments between moments in adjacent Co planes [24–28]. The dominant interactions are found to be FM from the positive Weiss temperature obtained by fitting the magnetic susceptibility χ vs T measurements above T_N by the Curie-Weiss law [25–27], indicating that interplane AFM interactions responsible for the **A**-type AFM ordering are much weaker than the intraplane FM ones. Electronic structure calculations are consistent with the itinerant **A**-type AFM ground state and the small ordered moment [29]. Spin-flop transitions in single crystals of $CaCo_{2-y}As_2$ with the magnetic field H applied parallel to the c axis occur at $H_{SF} \sim 3.5$–3.7 T [25,26,30,31]. On the other hand, metallic $SrCo_2As_2$ exhibits no magnetic transitions vs T [32]. However, single-crystal $\chi(T)$ data for both c-axis and ab-plane magnetic field alignments show broad maxima at $T \approx 115$ K, suggesting the presence of dynamic AFM correlations. Indeed, inelastic neutron scattering measurements on single crystals revealed strong AFM correlations with the same stripe wave vector as seen in the parent and doped Fe-based AFe_2As_2 compounds [33].

In view of the **A**-type AFM of $CaCo_{2-y}As_2$ where strong FM correlations dominate and the contrasting strong AFM correlations in paramagnetic (PM) $SrCo_2As_2$ detected by neutron scattering, studies of the magnetic properties of $Ca_{1-x}Sr_xCo_{2-y}As_2$ crystals have the potential to reveal additional interesting physics. This system is metallic with the $ThCr_2Si_2$-type structure over the entire composition

range $0 \leq x \leq 1$ [22]. On the basis of magnetization vs magnetic field $M(H)$ and electrical resistivity measurements on Ca$_{1-x}$Sr$_x$Co$_{2-y}$As$_2$ crystals, the authors of Ref. [22] inferred A-type c-axis AFM for $0 \leq x \lesssim 0.15$ (AFMI), a c-axis FM phase for $0.15 \lesssim x \lesssim 0.27$, ab-plane AFM ordering for $0.27 \lesssim x \lesssim 0.42$ (AFMII), and a PM phase for $0.42 \lesssim x \leq 1$, with one crystal defining each of the FM and AFMII phase regions. A first-order transition from the cT to the uncollapsed-tetragonal (ucT) structure at $x \approx 0.4$ was suggested from the variation in the c-axis lattice parameter with x, which the authors suggested was important to the evolution of the magnetic structure with x [22].

Here we present a detailed study of the magnetic properties and phase diagram of the Ca$_{1-x}$Sr$_x$Co$_{2-y}$As$_2$ system that was carried out using ten single crystals with Sr compositions in the range $0 \leq x \leq 0.52$. For crystals with x in the intermediate crossover regime $0.2 \lesssim x \lesssim 0.3$ between the c-axis and ab-plane AFM moment orientations of the AFMI and AFMII phases, respectively, we discovered that $\chi_{ab}(T)$ exhibits a cusp at the magnetic ordering temperature typical of an ab-plane AFM transition, whereas the response of $\chi_c(T)$ and $M_c(H)$ to a c-axis field is extremely soft, suggesting instead a c-axis FM structure in this region as proposed in Ref. [22]. This divergence between the magnetic responses in the two field directions is highly anomalous. We also established that the moment realignment between the AFMI and AFMII phases results from a continuous composition-induced evolution of the magnetocrystalline anisotropy field from c-axis to ab-plane orientations and that the structural parameters vs x, $T_N(x)$ [defined as the cusp temperature in $\chi_{ab}(T)$], the low-T saturation moment $\mu_{sat}(x)$, and the effective moment $\mu_{eff}(x)$ in the PM state at $T > T_N$ all vary continuously with x for $0 \leq x \leq 0.45$. Details about the crystal growth together with elemental analyses and single-crystal structure determinations are given in Ref. [34]. $M(H, T)$ and $C_p(T)$ data were obtained using a Quantum Design Magnetic Properties Measurement System and Physical Properties Measurement System, respectively.

Shown in Fig. 1 are zero-field-cooled $\chi(T) \equiv M(T)/H$ data in $H = 0.1$ T applied both parallel and perpendicular to the c axis for $0 \leq x \leq 0.52$. For $x = 0$ to 0.15 one sees that $\chi_c \ll \chi_{ab}$ for $T \ll T_N \approx 63$ K, suggesting A-type collinear c-axis ordering as already established for $x = 0$. Here χ_{ab} exhibits a cusp at $T \equiv T_N$ and is approximately independent of T below T_N, as expected for an AFM transition. Even though T_N is nearly independent of x in this region, the magnetic system becomes very soft against c-axis fields as reflected by the sharp peak in χ_c for $x \leq 0.15$ that appears to be diverging with increasing x. This is also reflected by the order of magnitude increase in the maximum χ_c from $x = 0$ to $x = 0.19$ in Fig. 1. For $x = 0.33$ a T-induced spin-reorientation transition appears to occur at about 50 K. This plot is similar to that for
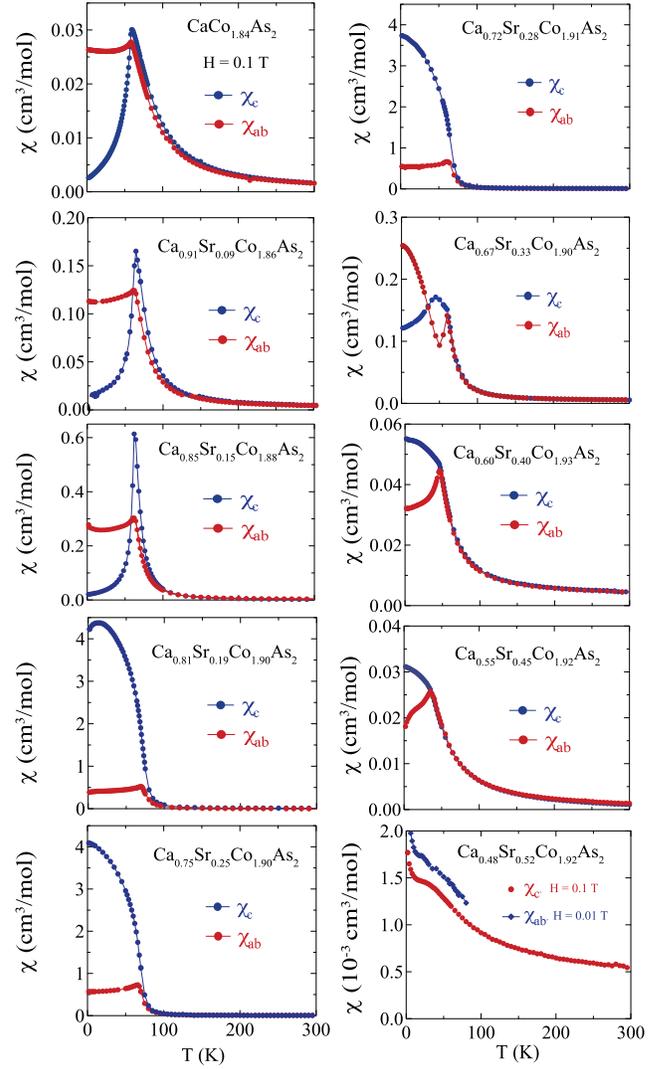

FIG. 1. Zero-field-cooled magnetic susceptibility χ of Ca$_{1-x}$Sr$_x$Co$_{2-y}$As$_2$ crystals vs T in $H = 0.1$ T applied in the ab plane (χ_{ab}) and along the c axis (χ_c). Note the large changes in the ordinate scales vs x.

$x = 0.34$ reported in Ref. [22]. For $x = 0.40$ and 0.45, the χ values at low T decrease to small values, and the $\chi(T)$ data suggest ab-plane AFM ordering. Finally, for $x = 0.52$, a PM behavior is observed. As a point of reference, the magnetic-dipole interaction between local moments on a simple-tetragonal lattice with $c/a \approx 3.65$ as in CaCo$_{2-y}$As$_2$ predicts that the ordered moments should lie in the ab plane [40].

To clarify the origins of the behaviors in Fig. 1 and the magnetic ground state vs x, we carried out isothermal $M(H)$ measurements on the same set of ten crystals at $T = 2$ K and the results are shown in Fig. 2. As expected for A-type c-axis collinear AFM ordering for small x [24], the crystals with $x = 0$, 0.09, and 0.15 show clear evidence for first-order field-induced spin-flop (SF) transitions for $H \| c$, where the SF fields decrease from $H_{SF} \approx 3.7$ T

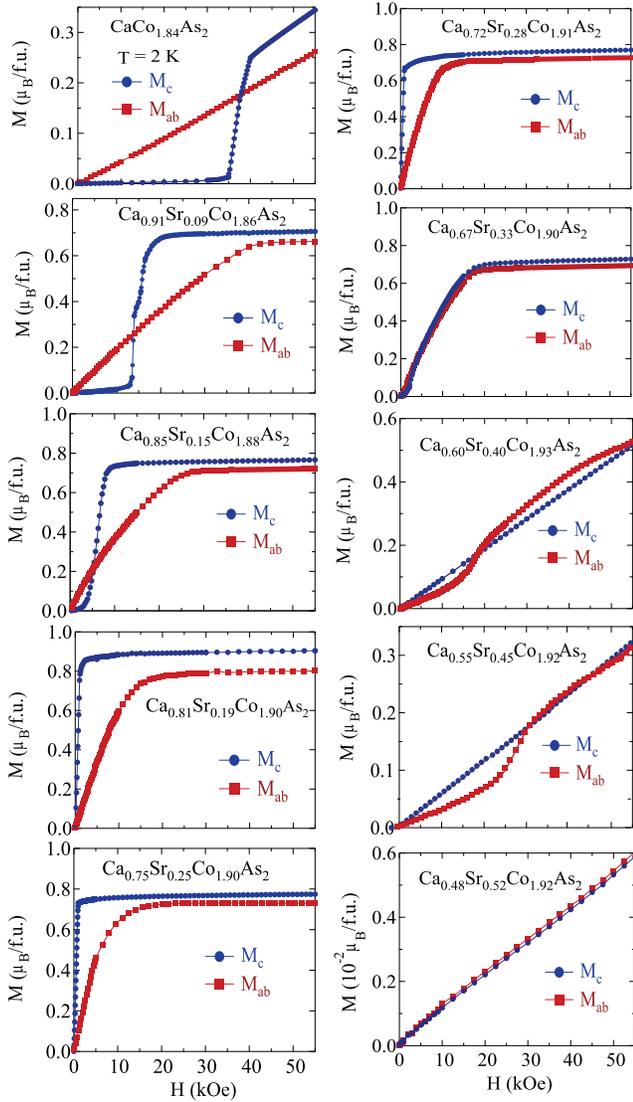FIG. 2. $M(H)$ data for $Ca_{1-x}Sr_xCo_{2-y}As_2$ crystals at $T = 2$ K for H applied in the ab plane (M_{ab}) and along the c axis (M_c).

FIG. 3. $M_c(H)$ data for $H \leq 1500$ Oe at $T = 2$ K for three crystals of $Ca_{1-x}Sr_xCo_{2-y}As_2$.

for $x = 0$ to $H_{SF} \approx 0.6$ T for $x = 0.15$. The measured saturation moment μ_{sat} values at high fields are in the narrow range of ≈ 0.35 to ≈ 0.42 μ_B/Co for $0.09 \leq x \leq 0.33$. Additional magnetic data in Ref. [34] show that the effective moment μ_{eff} per Co atom in the PM state is also nearly independent of x for $0 \leq x \leq 0.45$.

Figure 2 indicates that at 2 K, $H_{SF} \approx 0$ for $x = 0.19, 0.25$ and 0.28, where T_N from Fig. 1 and Ref. [34] decreases continuously from 71 to 63 K over this composition range. At the same time, the slope of $M_c(H)$ at low fields for these compositions remains high. To examine this low-field dependence in more detail, expanded plots of $M_c(H)$ for $0 \leq H \leq 1500$ Oe are shown in Fig. 3. For $x = 0.19$ a weak SF transition is detected at $H_{SF} \approx 100$ Oe. One also sees in Fig. 3 that the rapid increase in M_c with H at low fields for $H \| c$ in Fig. 2 is linear in H with nearly the same slope for the three compositions. This effect is expected if
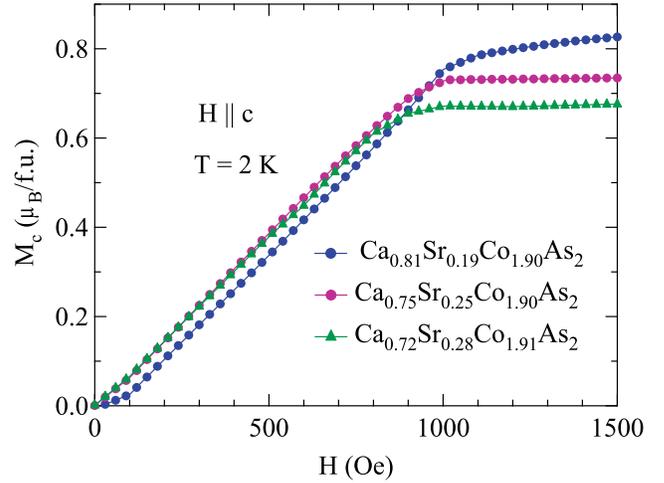
the slope is limited by demagnetization effects. The dimensionless volume susceptibility of the $M_c(H)$ data in Fig. 3 up to $H = 800$ Oe for all three compositions is $\chi_c \equiv dM_c/dH \approx 0.077$. This value is about the same as the value $\chi_c = 1/4\pi \approx 0.080$ expected if M_c/H in the absence of demagnetization effects is so large that the observed value is limited by the demagnetization factor [40]. Hence the magnetic response along the c axis is extremely soft for $x = 0.19, 0.25$ and 0.28, which may be expected if these compositions are in a crossover region in the magnetocrystalline anisotropy field from being parallel to perpendicular to the c axis. The rapid growth with increasing x of the sharp peak in $\chi_c(T_N)$ for $x = 0.09$ and 0.15 in Fig. 1 is an additional indication of the growth of strong FM fluctuations.

The crystal with Sr composition $x = 0.33$ is unique among the ten $Ca_{1-x}Sr_xCo_{2-y}As_2$ crystals, because it exhibits a T-induced spin-reorientation transition as revealed by the χ data for this composition in Fig. 1. On cooling below its $T_N = 60$ K, the χ anisotropy indicates that the ordered moments are oriented within the ab plane. But then on further cooling to the range $T = 45$ to 50 K, the ordered-moment direction switches from the ab plane to the c axis and remains so down to 2 K. This spin-reorientation transition is confirmed by the anisotropy of the magnetization isotherms in Fig. 4, which show a weak metamagnetic transition at about 2.5 kOe at 50 K for **H** aligned in the ab plane, and instead a spin-flop transition at $H_{SF} \approx 2.4$ kOe at 2 K for **H** aligned along the c axis.

The $M_c(H)$ behavior for $x = 0.2$ in Ref. [22] is about the same as we see for $x = 0.19, 0.25$ and 0.28 in Fig. 2, which those authors interpreted as a c-axis FM region of the phase diagram. However, the $\chi_{ab}(T)$ behaviors in Fig. 1 for $x = 0.19, 0.25$ and 0.28 instead suggest that the magnetic structure is AFM in this region. The magnetic behaviors of $ThCo_{1.2}Cu_{0.8}Sn_2$ with a different crystal structure [41] are
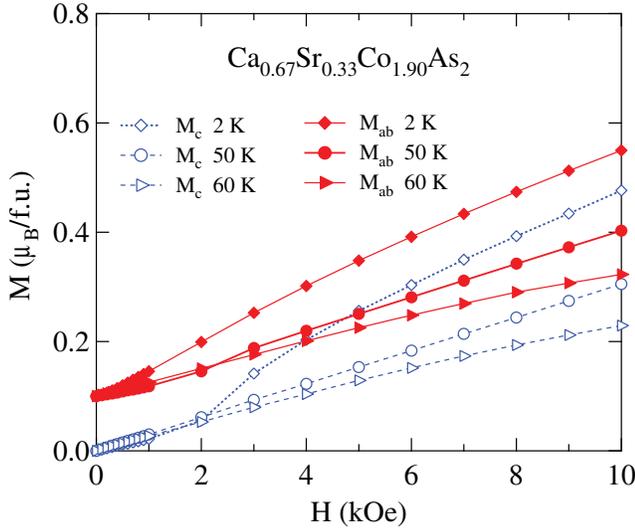
FIG. 4. Magnetization M vs applied magnetic field H for fields aligned along the c axis (open symbols) and ab plane (filled symbols), each at 2, 50 and 60 K. The ab-plane data are offset vertically by 0.1 μ_B/f.u. for clarity.

FIG. 5. Magnetic phase diagram of the $Ca_{1-x}Sr_xCo_{2-y}As_2$ system vs x at $T = 2$ K, containing the c-axis AFMI (A-type), ab-plane AFMII and PM phases. The crossover region in yellow and the AFMII phase have unknown structures. Plotted are the spin-flop field H_{SF} with $H\|c$ for $x < 0.2$ and the metamagnetic transition field H_{mm} with $H\|ab$ for $x > 0.3$ (left-hand ordinates). Also shown is $T_N(x)$ (right-hand ordinate), defined as the cusp temperatures in the $\chi_{ab}(T)$ data in Fig. 1.

similar to our data for $Ca_{1-x}Sr_xCo_{2-y}As_2$ in the crossover regime with $x \approx 0.2$ to 0.3, but no discussion or interpretation of the data was given.

At larger x values of 0.40 and 0.45, metamagnetic transitions occur at 2 K with H applied in the ab plane instead of along the c axis which indicates ab-plane AFM ordering (AFMII) as suggested for $x = 0.34$ in Ref. [22]. We interpret this as resulting from a crossover in the anisotropy field from being parallel to the c axis for $0 \le x \lesssim 0.2$ to perpendicular to the c axis for $0.35 \lesssim x \lesssim 0.45$. If this ordering is collinear, one expects AFM domains to occur in the ab plane with orthogonal easy axes, corresponding to an extrinsic noncollinear AFM structure. The $\chi_{ab}(T)$ data for $x = 0.40$ and 0.45 in Fig. 1, which remain relatively large with respect to $\chi_c(T)$ at $T \ll T_N$, suggest that the AFM structure in this x range is either extrinsically or intrinsically noncollinear [42–44]. In either case, the high-field $M_{ab}(H)$ behavior is not straightforward to interpret. Therefore we denote the metamagnetic transition field for $x = 0.40$ and 0.45 as H_{mm} instead of H_{SF}. One sees from Fig. 2 that H_{mm} increases from ≈ 1.7 T for $x = 0.40$ to ≈ 2.8 T for $x = 0.45$ before becoming irrelevant in the PM state for $x \ge 0.52$.

We have also carried out heat capacity $C_p(T)$ measurements on the $Ca_{1-x}Sr_xCo_{2-y}As_2$ crystals in $H = 0$ [34]. As in the $C_p(T)$ measurements for $x = 0$ in Ref. [25], we see no distinct anomalies in C_p at T_N for any of the $Ca_{1-x}Sr_xCo_{2-y}As_2$ crystals. The low-T data indicate substantial Sommerfeld coefficients γ, suggesting enhanced densities of states at the Fermi energy.

The ground-state magnetic phase diagram of the $Ca_{1-x}Sr_xCo_{2-y}As_2$ system derived from the measurements at $T = 2$ K of H_{SF} and H_{mm} vs x is shown in Fig. 5, where $T_N(x)$ is also plotted. The AFMI phase for $0 \le x \lesssim 0.2$ is

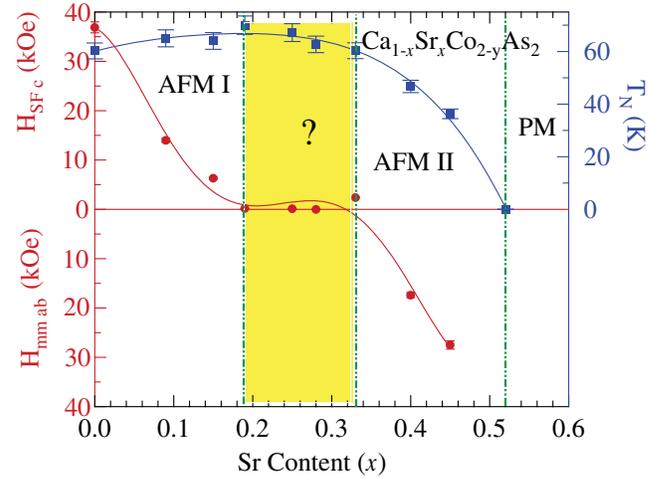an A-type AFM with c-axis moment alignment. The AFM structure in the anisotropy crossover region $0.2 \lesssim x \lesssim 0.3$ is unknown. Then an AFMII phase with unknown AFM structure with the ordered moments aligned in the ab plane occurs for $x = 0.40$ and 0.45, followed by a PM region for $x \ge 0.52$. From the $\chi(T)$ data for $x = 0.40$ and 0.45 in Fig. 1 we infer that the AFMII structure is intrinsically noncollinear or else extrinsically noncollinear due to multiple collinear AFM domains aligned in the ab plane. Since T_N, μ_{sat} and μ_{eff} over the region $0.2 \lesssim x \lesssim 0.3$ do not change appreciably [34], one might infer that a continuous tilting of the ordered moment from c-axis to ab-plane orientation occurs over this region. However, this seems unlikely since the magnetic data for this region do not provide clear evidence for it and the magnetism is itinerant.

In summary, the magnetic and thermal properties of $Ca_{1-x}Sr_xCo_{2-y}As_2$ single crystals with $0 \le x \le 0.52$ were studied and the magnetic phase diagram at $T = 2$ K was constructed. We confirm a collinear c-axis AFM phase at small $x \lesssim 0.2$ and an ab-plane AFM phase at large $x = 0.40$ and 0.45 [22]. Our major result is the observation of AFM-like transitions from $\chi_{ab}(T)$ coexisting with strong FM-like c-axis correlations from $\chi_c(T)$ and $M_c(H)$ data in the crossover region $0.2 \lesssim 0.3$ between these two phases, an anomalous dichotomy. We also find continuous evolutions with x from $x = 0$ to 0.52 of the crystal structure, of the anisotropy field at $T = 2$ K which results in the composition-induced ordered-moment reorientation between the c-axis AFMI and ab-plane AFMII phases, and of the ordered and effective moments [34].

An important feature of this system is that it is isoelectronic and isostructural over the entire composition range $0 \leq x \leq 1$, which may simplify theoretical analyses. The itinerant-electron AFM $Ca_{1-x}Sr_xCo_{2-y}As_2$ system provides fertile ground for additional experimental and theoretical investigations that may also shed light on the origin of the temperature-induced ordered-moment realignments of the AFM phases in the hole-underdoped 122-type FeAs-based high-T_c superconductors.

[1] D. C. Johnston, The puzzle of high temperature superconductivity in layered iron pnictides and chalcogenides, Adv. Phys. **59**, 803 (2010).

[2] G. R. Stewart, Superconductivity in iron compounds, Rev. Mod. Phys. **83**, 1589 (2011).

[3] E. Dagotto, The unexpected properties of alkali metal iron selenide superconductors, Rev. Mod. Phys. **85**, 849 (1913).

[4] R. M. Fernandes, A. V. Chubukov, and J. Schmalian, What drives nematic order in iron-based superconductors?, Nat. Phys. **10**, 97 (2014).

[5] P. Dai, Antiferromagnetic order and spin dynamics in iron-based superconductors, Rev. Mod. Phys. **87**, 855 (2015).

[6] Q. Si, R. Yu, and E. Abrahams, High-temperature superconductivity in iron pnictides and chalcogenides, Nat. Rev. Mater. **1**, 1 (2016).

[7] S. Avci, O. Chmaissem, J. M. Allred, S. Rosenkranz, I. Eremin, A. V. Chubukov, D. E. Bugaris, D. Y. Chung, M. G. Kanatzidis, J.-P. Castellan, J. A. Schlueter, H. Claus, D. D. Khalyavin, P. Manuel, A. Daoud-Aladine, and R. Osborn, Magnetically driven suppression of nematic order in an iron-based superconductor, Nat. Commun. **4**, 3845 (2014).

[8] F. Waßer, A. Schneidewind, Y. Sidis, S. Wurmehl, S. Aswartham, B. Büchner, and M. Braden, Spin reorientation in $Ba_{0.65}Na_{0.35}Fe_2As_2$ studied by single-crystal neutron diffraction, Phys. Rev. B **91**, 060505(R) (2015).

[9] A. E. Böhmer, F. Hardy, L. Wang, T. Wolf, P. Schweiss, and C. Meingast, Superconductivity-induced re-entrance of the orthorhombic distortion in $Ba_{1-x}K_xFe_2As_2$, Nat. Commun. **6**, 7911 (2015).

[10] B. P. P. Mallett, Yu. G. Pashkevich, A. Gusev, Th. Wolf, and C. Bernhard, Muon spin rotation study of the magnetic structure in the tetragonal antiferromagnetic state of weakly underdoped $Ba_{1-x}K_xFe_2As_2$, Europhys. Lett. **111**, 57001 (2015).

[11] B. P. P. Mallett, P. Marsik, M. Yazdi-Rizi, Th. Wolf, A. E. Böhmer, F. Hardy, C. Meingast, D. Munzar, and C. Bernhard, Infrared Study of the Spin Reorientation Transition and Its Reversal in the Superconducting State in Underdoped $Ba_{1-x}K_xFe_2As_2$, Phys. Rev. Lett. **115**, 027003 (2015).

[12] J. M. Allred, K. M. Taddei, D. E. Bugaris, M. J. Krogstad, S. H. Lapidus, D. Y. Chung, H. Claus, M. G. Kanatzidis, D. E. Brown, J. Kang, R. M. Fernandes, I. Eremin, S. Rosenkranz, O. Chmaissem, and R. Osborn, Double-Q spin-density wave in iron arsenide superconductors, Nat. Phys. **12**, 493 (2016).

[13] K. M. Taddei, J. M. Allred, D. E. Bugaris, S. Lapidus, M. J. Krogstad, R. Stadel, H. Claus, D. Y. Chung, M. G. Kanatzidis, S. Rosenkranz, R. Osborn, and O. Chmaissem, Detailed magnetic and structural analysis mapping a robust magnetic C_4 dome in $Sr_{1-x}Na_xFe_2As_2$, Phys. Rev. B **93**, 134510 (2016).

[14] K. M. Taddei, J. M. Allred, D. E. Bugaris, S. H. Lapidus, M. J. Krogstad, H. Claus, D. Y. Chung, M. G. Kanatzidis, R. Osborn, S. Rosenkranz, and O. Chmaissem, Observation of the magnetic C_4 phase in $Ca_{1-x}Na_xFe_2As_2$ and its universality in the hole-doped 122 superconductors, Phys. Rev. B **95**, 064508 (2017).

[15] J. Kang, X. Wang, A. V. Chubukov, and R. M. Fernandes, Interplay between tetragonal magnetic order, stripe magnetism, and superconductivity in iron-based materials, Phys. Rev. B **91**, 121104(R) (2015).

[16] M. N. Gastiasoro and B. M. Andersen, Competing magnetic double-Q phases and superconductivity-induced reentrance of C_2 magnetic stripe order in iron pnictides, Phys. Rev. B **92**, 140506(R) (2015).

[17] M. H. Christensen, J. Kang, B. M. Andersen, I. Eremin, and R. M. Fernandes, Spin reorientation driven by the interplay between spin-orbit coupling and Hund's rule coupling in iron pnictides, Phys. Rev. B **92**, 214509 (2015).

[18] R. M. Fernandes, S. A. Kivelson, and E. Berg, Vestigial chiral and charge orders from bidirectional spin-density waves: Application to the iron-based superconductors, Phys. Rev. B **93**, 014511 (2016).

[19] M. Hoyer, R. M. Fernandes, A. Levchenko, and J. Schmalian, Disorder-promoted C_4-symmetric magnetic order in iron-based superconductors, Phys. Rev. B **93**, 144414 (2016).

[20] D. D. Scherer, I. Eremin, and B. M. Andersen, Collective magnetic excitations of C_4-symmetric magnetic states in iron-based superconductors, Phys. Rev. B **94**, 180405(R) (2016).

[21] M. H. Christensen, B. M. Andersen, and P. Kotetes, Unravelling incommensurate magnetism and the path to intrinsic topological superconductivity in iron-pnictides, arXiv:1612 .07633.

[22] J. J. Ying, J. C. Liang, X. G. Luo, Y. J. Yan, A. F. Wang, P. Cheng, G. J. Ye, J. Q. Ma, and X. H. Chen, The magnetic phase diagram of $Ca_{1-x}Sr_xCo_{2-y}As_2$ single crystals, Europhys. Lett. **104**, 67005 (2013).

[23] For a review of collapsed and uncollapsed tetragonal phases, see Sec. VII in V. K. Anand, P. Kanchana Perera, A. Pandey, R. J. Goetsch, A. Kreyssig, and D. C. Johnston, Crystal growth and physical properties of $SrCu_2As_2$, $SrCu_2Sb_2$, and $BaCu_2Sb_2$, Phys. Rev. B **85**, 214523 (2012).

[24] D. G. Quirinale, V. K. Anand, M. G. Kim, A. Pandey, A. Huq, P. W. Stephens, T. W. Heitmann, A. Kreyssig,

R. J. McQueeney, D. C. Johnston, and A. I. Goldman, Crystal and magnetic structure of $CaCo_{1.86}As_2$ studied by x-ray and neutron diffraction, Phys. Rev. B **88**, 174420 (2013).

[25] V. K. Anand, R. S. Dhaka, Y. Lee, B. N. Harmon, A. Kaminski, and D. C. Johnston, Physical properties of metallic antiferromagnetic $CaCo_{1.86}As_2$ single crystals, Phys. Rev. B **89**, 214409 (2014).

[26] J. J. Ying, Y. J. Yan, A. F. Wang, Z. J. Xiang, P. Cheng, G. J. Ye, and X. H. Chen, Metamagnetic transition in $Ca_{1-x}Sr_xCo_{2-y}As_2$ ($x = 0$ and 0.1) single crystals, Phys. Rev. B **85**, 214414 (2012).

[27] B. Cheng, B. F. Hu, R. Y. Chen, G. Xu, P. Zheng, J. L. Luo, and N. L. Wang, Electronic properties of $3d$ transitional metal pnictides: A comparative study by optical spectroscopy, Phys. Rev. B **86**, 134503 (2012).

[28] W. T. Jayasekara, A. Pandey, A. Kreyssig, N. S. Sangeetha, A. Sapkota, K. Kothapalli, V. K. Anand, W. Tian, D. Vaknin, D. C. Johnston, R. J. McQueeney, A. I. Goldman, and B. G. Ueland, Suppression of magnetic order in $CaCo_{1.86}As_2$ with Fe substitution: Magnetization, neutron diffraction, and x-ray diffraction studies of $Ca(Co_{1-x}Fe_x)_yAs_2$, Phys. Rev. B **95**, 064425 (2017).

[29] M. A. Korotin, Z. V. Pchelkina, N. A. Skorikov, V. I. Anisimov, and A. O. Shorikov, Investigation of electronic structure and magnetic properties of $CaCo_{1.86}As_2$ within the CPA method, J. Phys.: Condens. Matter **27**, 045502 (2015).

[30] B. Cheng, B. F. Hu, R. H. Yuan, T. Dong, A. F. Fang, Z. G. Chen, G. Xu, Y. G. Shi, P. Zheng, J. L. Luo, and N. L. Wang, Field-induced spin-flop transitions in single-crystalline $CaCo_2As_2$, Phys. Rev. B **85**, 144426 (2012). The double spin-flop transitions seen in this work are likely due to inhomogeneity in the crystal studied.

[31] W. Zhang, K. Nadeem, H. Xiao, R. Yang, B. Xu, H. Yang, and X. G. Qiu, Spin-flop transition and magnetic phase diagram in $CaCo_2As_2$ revealed by torque measurements, Phys. Rev. B **92**, 144416 (2015).

[32] A. Pandey, D. G. Quirinale, W. Jayasekara, A. Sapkota, M. G. Kim, R. S. Dhaka, Y. Lee, T. W. Heitmann, P. W. Stephens, V. Ogloblichev, A. Kreyssig, R. J. McQueeney, A. I. Goldman, A. Kaminski, B. N. Harmon, Y. Furukawa,

and D. C. Johnston, Crystallographic, electronic, thermal, and magnetic properties of single-crystal $SrCo_2As_2$, Phys. Rev. B **88**, 014526 (2013).

[33] W. Jayasekara, Y. Lee, A. Pandey, G. S. Tucker, A. Sapkota, J. Lamsal, S. Calder, D. L. Abernathy, J. L. Niedziela, B. N. Harmon, A. Kreyssig, D. Vaknin, D. C. Johnston, A. I. Goldman, and R. J. McQueeney, Stripe Antiferromagnetic Spin Fluctuations in $SrCo_2As_2$, Phys. Rev. Lett. **111**, 157001 (2013).

[34] See Supplemental Material at http://link.aps.org/supplemental/10.1103/PhysRevLett.119.257203 for crystal growth details, chemical composition analyses, single-crystal structure determinations, heat capacity, magnetization and magnetic susceptibility data, and includes Refs. [35–39].

[35] APEX3, Bruker AXS Inc., Madison, Wisconsin, USA, 2015.

[36] SAINT, Bruker AXS Inc., Madison, Wisconsin, USA, 2015.

[37] L. Krause, R. Herbst-Irmer, G. M. Sheldrick, and D. Stalke, Comparison of silver and molybdenum microfocus x-ray sources for single-crystal structure determination, J. Appl. Crystallogr. **48**, 3 (2015).

[38] G. M. Sheldrick, SHELTX—Integrated space-group and crystal-structure determination, Acta Crystallogr. A **71**, 3 (2015).

[39] G. M. Sheldrick, Crystal structure refinement with SHELXL, Acta Crystallogr. C **71**, 3 (2015).

[40] D. C. Johnston, Magnetic dipole interactions in crystals, Phys. Rev. B **93**, 014421 (2016).

[41] P. F. S. Rosa, T. M. Garitezi, Z. Fisk, and P. G. Pagliuso, $3d$ magnetism in $ThCo_2Sn_2$ single crystals, J. Phys.: Conf. Ser. **592**, 012053 (2015).

[42] D. C. Johnston, Magnetic Susceptibility of Collinear and Noncollinear Heisenberg Antiferromagnets, Phys. Rev. Lett. **109**, 077201 (2012).

[43] D. C. Johnston, Unified molecular field theory for collinear and noncollinear Heisenberg antiferromagnets, Phys. Rev. B **91**, 064427 (2015).

[44] N. S. Sangeetha, E. Cuervo-Reyes, A. Pandey, and D. C. Johnston, $EuCo_2P_2$: A model molecular-field helical Heisenberg antiferromagnet, Phys. Rev. B **94**, 014422 (2016).